RSC Advances

ROYAL SOCIETY OF CHEMISTRY

www.rsc.org/advances

RSC Advances

PAPER

Palladium dispersed in three-dimensional polyaniline networks as the catalyst for hydrogen peroxide electro-reduction in acidic medium

Received 00th January 20xx,
Accepted 00th January 20xx

DOI: 10.1039/x0xx00000x

www.rsc.org/

Fen Guo, Ke Ye*, Xiaomei Huang, Yinyi Gao, Kui Cheng, Guiling Wang and Dianxue Cao*

A novel Pd/polyaniline/CFC electrode is prepared by electroless deposition of palladium (Pd) onto three-dimensional polyaniline networks. The polyaniline matrix on carbon fiber cloth (CFC) in reduction state is electro-synthesized by cyclic voltammetry with lower vertex potential of -0.4 V vs. Ag/AgCl. The particle size of Pd coated on polyaniline chains is gradiently distributed. The as-prepared Pd/polyaniline/CFC electrode is characterized by scanning electron microscopy (SEM), Fourier transform infrared spectroscopy (FITR) and X-ray diffraction (XRD). Hydrogen peroxide (H_2O_2) electro-reduction reaction in H_2SO_4 solutions on the Pd/polyaniline/CFC electrode is investigated by cyclic voltammetry (CV), linear sweep voltammetry (LSV), chronoamperometry (CA) and electrochemical impedance spectroscopy (EIS). Results reveal that the electrode exhibited high catalytic activity and excellent stability in the strong oxidizing solution of H_2O_2 and H_2SO_4. Polyaniline itself shows electro-catalytic activity towards H_2O_2 to some extent involving chemical-electrochemical (C-E) coupling mechanism.

1. Introduction

Fuel cell (FC), distinguished from other rechargeable secondary power, such as Li ion battery and supercapacitor[1–3], is a kind of power source that can constantly generate electricity[4–7]. FCs convert chemical energy efficiently into electrical energy without the limitation of Carnot cycle. Hydrogen, methane and alcohols are the three main fuel resources for FCs. Compared with the abundant resources of anode fuel, there is only one kind of universal oxidant, that is, oxygen. Oxygen can be extracted directly from air, however, its electro-reduction activity depends very closely on platinum catalyst. The gas needs extra humidifying apparatus and high-strength pumping to achieve good FC performance. For the past few years, hydrogen peroxide (H_2O_2) was used as the oxidant for metal semi-fuel cell[8], direct borohydride[9], direct hydrogen peroxide[10] and hydrazine[11] fuel cell. Using H_2O_2 instead of O_2 will make FC system more compact, and especially helps FCs work in the oxygen-free underwater and outer space.

Catalysts with high specific surface area supply more active sites for H_2O_2 electro-reduction[12, 13]. Commercial Pd/C and Pt/C catalysts are obtained by chemically reducing Pd or Pt on carbon black to maintain their nano-particle morphology. Others favored graphene which has the thickness of a few nanometers, and then dispersed noble metal particles on it for better catalytic applications. Polyaniline, synthesized by simple process, generally has various nanoscale structures, such as particle, fiber, tube and sphere[14–17]. Lamy et al.[18] prepared polyaniline on glassy carbon stationary electrode by cyclic voltammetric technique, afterwards, potentiostatically electrodeposited platinum on polyaniline film to design a Pt/polyaniline electrode for oxygen reduction reaction. The supply of electrodeposition potential for depositing Pt would change the redox states and impair the electrical conductivity of polyaniline, invalidating the composite electrode. Stejskal et al.[19] adopted silver nitrate as oxidant to oxidize aniline to polyaniline, and in the meantime silver ions were reduced to silver coated on polyaniline. Li and the co-workers[20] synthesized Au/polyaniline through mutual redox of aniline vapor and $HAuCl_4$ aqueous solution for the oxidation and sensing of ascorbic. The ways that using noble metal compounds as oxidant to chemically make noble metal/ polyaniline electrode need extra processes, like mixing noble metal/polyaniline powder with binder, coating on a support for testing, etc. The binder would lower the conductivity of electrode and, for long duration tests, the electrode powders may fall off from the support in the aqueous electrolyte[21–23].

Electro-synthesized polyaniline assisted by CV technique has different redox states and conductivity by selecting potential range of CV[24, 25]. Fig. 1 illustrates the common three redox states of polyaniline. Emeraldine has the highest conductivity while lencomeraldine and pernigraniline are electrically isolated[26]. If as-prepared polyaniline on a support

Key Laboratory of Superlight Materials and Surface Technology of Ministry of Education, College of Materials Science and Chemical Engineering, Harbin Engineering University, Harbin, 150001, P.R. China. E-mail addresses: yeke@hrbeu.edu.cn (K. Ye); caodianxue@hrbeu.edu.cn (D. Cao)

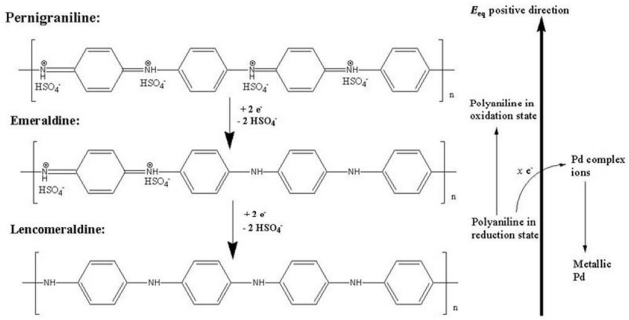

Fig. 1 Schematic illustration of the three redox states of polyaniline and mutual redox between Pd(II) and polyaniline.

is in reduction state, and can thermodynamically reduce noble metal complex ions, a binder-free noble metal/polyaniline electrode would be successfully achieved. Moreover, the oxidation of polyaniline cannot go too far and thus, the mutual redox between formed polyaniline and noble metal compounds has less severe influence on the electrode conductivity.

In this work, Pd was electrolessly deposited on polyaniline fibrils by the reduction-state polyaniline itself. The Pd/polyaniline/CFC electrode was introduced to catalyze H_2O_2 electro-reduction because of the synergistic properties of high-surface-area polyaniline doping-dedoping in H_2SO_4 and Pd electro-reduction towards H_2O_2. The obtained electrode owns unique three-dimensional network structure, which enables easy access of the fuel and product into or out from the catalytic active sites. Results indicated that the Pd/polyaniline/CFC electrode for H_2O_2 electro-reduction exhibited high catalytic activity and excellent stability.

2. Experimental

2.1. Preparation of the polyaniline/CFC and Pd/polyaniline/CFC electrodes

Aniline monomers were in-situ electro-polymerized on CFC by cyclic voltammetry in 1.0 mol L^{-1} sulfuric acid and 0.1 mol L^{-1} aniline (obtained from Aladdin Industrial Inc.) with a volume of 40 mL. Prior to use, the CFC (purchased from Shanghai Hesen Electric Inc.) was soaked in acetone for 20 minutes, washed copiously and preserved in milli-Q water (18.2 MΩ cm) successively. CFC was fixed between a pair of home-made titanium frame with an area of 1.0 × 1.0 cm exposed to the electrolyte. A platinum sheet (2.0 × 1.0 cm) and a saturated Ag/AgCl electrode (0.1981 V vs. SHE) were used as counter electrode and reference electrode, respectively. All potentials in this work were referred to this reference electrode except where noted. The electro-deposition solution was deoxygenated by bubbling ultrahigh purity N_2 for 10 min and maintained under N_2 atmosphere during polymerization. The CV polymerization was performed for 16 cycles with potential range of –0.4 V ~ 1 V at 50 mV s^{-1}.

To accomplish the electrolessly precipitated Pd/polyaniline/CFC modified electrode, the as-prepared polyaniline/CFC electrode was firstly washed by milli-Q water for several times in order to remove the anline monomer and oligomer, and then immediately transferred to the Pd complex ions (Pd(II)) solution under open circuit condition within the shortest possible lapse (typically 10 s). The Pd(II) solution is composed of 1.0 mmol L^{-1} $PdCl_2$ (Sinopharm Chemical Reagent Co., Ltd) and 20 mmol L^{-1} $HClO_4$. The mutual redox between Pd(II) and polyaniline was lasted for 2 hours. All experiments were carried out at ambient temperature (20°C ± 1°C).

2.2. Characterization of polyaniline / CFC and Pd / polyaniline / CFC electrodes

The morphologies of polyaniline/CFC and Pd/polyaniline/CFC electrodes were examined by a scanning electron microscope (SEM, JEOL JSM-6480). The structure was analyzed using an X-ray diffractometer (XRD, Rigaku TTR III) with Cu Kα radiation (λ=0.1514178 nm). The relevant groups of polyaniline before and after mutual redox with Pd(II) were investigated with Fourier transform infrared spectroscopy (FTIR, Equinos55, Bruker) using the potassium bromide pellet technique. The active materials of polyaniline and Pd, together with CFC were grinded into powder for FTIR characterizations.

2.3. Electrochemical measurements

Electrochemical measurements were performed in a conventional three-electrode or two-electrode electrochemical cell using a computerized potentiostat (Autolab PGSTAT302, Eco Chemie) controlled by GPES software. The open circuit potentials (E_{oc}) were monitored in a two-electrode system of Pd(II) solution with saturated Ag/AgCl electrode as reference electrode. For comparison, the E_{oc} of polyaniline electrode immersed in $PdCl_2$-free solution was also recorded. The equilibrium potentials of polyaniline/CFC electrode in 20 mmol L^{-1} $HClO_4$ and CFC electrode in Pd(II) solution were measured by potentiodynamic polarization at a scan rate of 1 mV s^{-1}. Electrochemical tests of cyclic voltammetry (CV), linear sweep voltammetry (LSV), chronoamperometry (CA) and electrochemical impedance spectroscopy (EIS) for H_2O_2 electro-reduction were performed in a typical three-electrode electrochemical cell. The obtained polyaniline/CFC or Pd/polyaniline/CFC electrode, platinum foil and a saturated Ag/AgCl electrode were employed as working electrode, counter electrode and reference electrode, respectively. The EIS tests were operated after an equilibrium time of 600 s at fixed potential. The frequency region was 100 kHz ~ 10 mHz with 5 mV potential amplitude.

3. Results and discussion

Fig. 2 shows the cyclic voltammograms for the polymerization of polyaniline on CFC. The first cycle shows an onset oxidation potential of aniline at approximately 0.8 V. The anodic and cathodic current response continuously increased, indicating the regular growth of polyaniline[27, 28]. The peaks during the potential range referred to various redox states of polyaniline, representing simultaneous electro-polymerization and dopping/dedopping process[29, 30]. In the former literatures[18, 24–26, 28, 30, 31], the lower vertex potential of CV for electro-

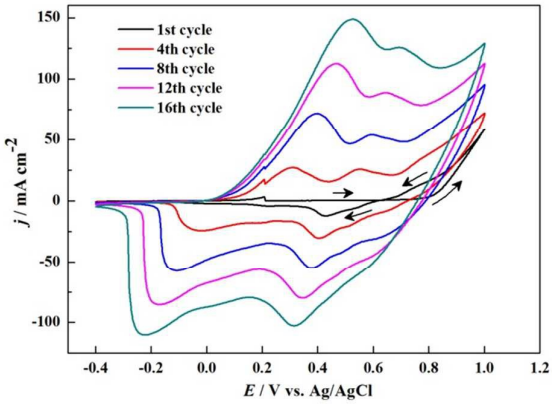

Fig. 2 Cyclic voltammograms for electro-polymerization of polyaniline on CFC in a solution containing 0.1 mol L^{-1} aniline and 1.0 mol L^{-1} sulfuric acid.

polymerization was mostly –0.16 V vs. Ag/AgCl (converted from the SCE scale in the references) or higher. For the sake of reduction state polyaniline (labeled as PAN_{re}), a more negative vertex potential of –0.4 V was set in this study. During the CV polymerization from –0.4 V to the higher vertex of 1.0 V, the color of polyaniline turning darker and darker from light green to black. The resulting polyaniline coated on CFC appeared a light green color. Before modification with Pd, the reaction feasibility of PAN_{re} oxidation and Pd(II) reduction was confirmed by their own equilibrium potentials. The two reactions are listed at below:

$$PAN_{re} - xe^- \rightleftarrows PAN_{ox} - xClO_4^- \quad (1)$$

$$x/2\ Pd(II) + xe^- \rightleftarrows x/2\ Pd(0) \quad (2)$$

In Eqs. (1), PAN_{ox} refers to the oxidation state of PAN_{re} after losing x electrons. Fig**.** 3a shows the Tafel plots derived from potentiodynamic polarization curves. Polyaniline/CFC electrode was immersed in perchloric acid solution, involving the proton doping/dedoping and simultaneous redox reaction as the potential sweeped (Eqs. (1)). CFC electrode was tested in perchloric acid and $PdCl_2$ solution, involving Pd(II)/Pd(0) redox reaction (Eqs. (2)). Based on the linear fittings of experimental data in Fig**.** 3a, the equilibrium potentials were 0.03 V for Eqs. (1) and 0.53 V for Eqs. (2). The oxidation reaction had a more negative equilibrium potential than reduction reaction, proving that Pd can be electrolessly deposited on the polyaniline synthesized in this work thermodynamically (as explained in the right of Fig. 1). The E_{oc}-t curves of polyaniline/CFC electrode in 20 mmol L^{-1} $HClO_4$ with and without 1.0 mmol L^{-1} $PdCl_2$ were demonstrated in figure 3b. The open circuit potential(E_{oc}) in $PdCl_2$-free solution shows a slightly upward tendency from 0.17 V at 0 s to 0.18 V at 7200 s, due to the weak oxidizability of dilute $HClO_4$ at room temperature. E_{oc} in $PdCl_2$-free solution was nearly unchanged, while that in $PdCl_2$ solution gradually rose up from 0.15 V at 0 s to 0.35 V at 2000 s. After that, the open circuit potential with time was kept in parallel with that in $PdCl_2$-free solution. This platform illustrated that after 2000s the mutual redox of Pd(II) and PAN_{re} finished. The long

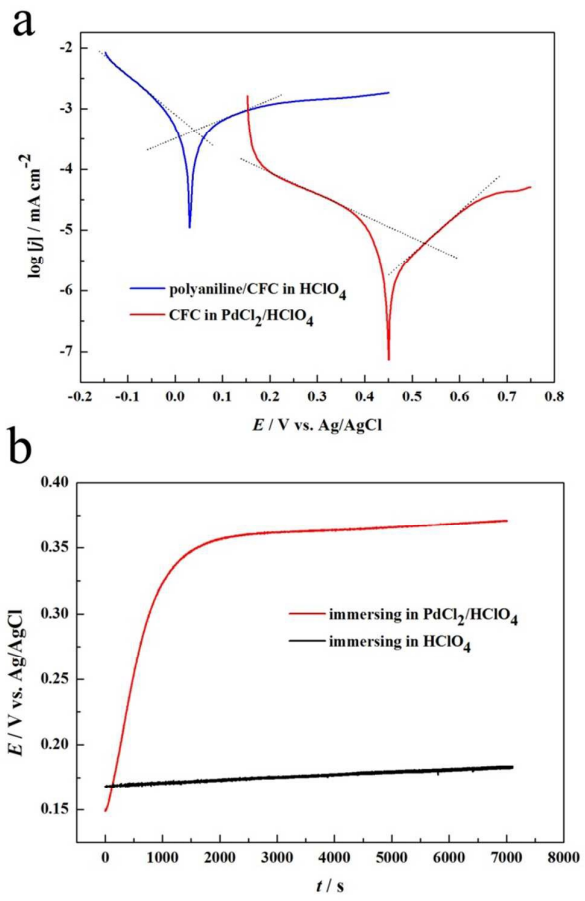

Fig. 3 (a) Tafel plots of CFC in 1.0 mmol L^{-1} $PdCl_2$ and 20 mmol L^{-1} $HClO_4$, of polyaniline/CFC in 20 mmol L^{-1} $HClO_4$ in the absence and presence of 1.0 mmol L^{-1} $PdCl_2$; (b) open circuit potential (E_{oc}) *vs.* time (t) plots of polyaniline/CFC electrode in 20 mmol L^{-1} $HClO_4$ with and without 1.0 mmol L^{-1} $PdCl_2$.

duration time of 2000 s and the slow rising between 0 s and 2000 s for the chemical redox reaction suggested that, there was probably a gradient diffusion of Pd(II) ions inside the polyaniline matrix where more active sites were available for the reduction of Pd(II) to Pd(0)[32].

Figs**.** 4a-c are the SEM micrographs of polyaniline and Pd/polyaniline composite supported on CFC. In Fig. 4a, the polyaniline synthesized by CV showed typically loose and fibrillary structure[25, 28, 33, 34]. The fibril diameter was ~150 nm on average. Many monofilament fibers cross-linked from each other to form the networks. Fig**.** 4b and c demonstrate the SEM images of Pd/polyaniline composite in low and high magnification. The much longer fibers in Figure 4b with a diameter of ~ 9 μm were carbon fibers. Based on previous reports[33, 34], the white spots, distinguished from darker CFC and polyaniline, were Pd centers. Zooming in the Pd/polyaniline/CFC, as shown in Fig**.** 4c, the Pd dispersion in polyaniline networks was inhomogeneous. Furthermore, the size of Pd particles was not uniform and even appeared to be

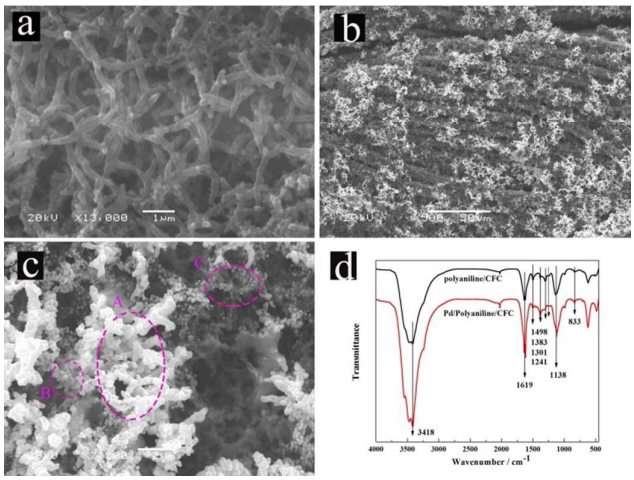

Fig. 4 SEM images of polyaniline before (a) and after (b and c) modification of Pd; (d) FTIR spectrums of polyaniline/CFC and Pd/polyaniline/CFC.

gradient distribution. A, B and C spots were where polyaniline faced to the Pd(II) solution from outside to inside. In the A spot, the Pd deposits nearly in-situ wrapped the polyaniline fibrils. In the B spot, the agglomeration of Pd occurred with clusters of particles on polyaniline fibrils. Pd particle at B spot had a size of 120 ~ 200 nm in diameter. Penetrating in the polyaniline networks to C spot, the Pd particle dotted sporadically on polyaniline fibrils had much smaller diameter of 50 ~ 80 nm. As Pd(II) ions diffused into polyaniline matrix for reduction, the concentration gradient would form from A to C spot, which undoubtedly made the size of Pd particle gradiently distribute.

Fig. 4d shows the FTIR spectrums of polyaniline before and after modification with Pd, respectively. The band of 3418 cm^{-1} represented N-H stretching mode[35]. The bands at 1383, 1301 and 1241 cm^{-1} were attributed to C-N stretching vibrations in QBQ, QBB, BBQ and BBB(Q denotes quinoid ring, B denotes benzenoid ring)[36, 37]. In the region of 1138 cm^{-1}, $-NH^{+}=$ stretching mode was observed. Out-of-plane deformations of C-H on 1,4-disubstituted benzenoid rings were located in the region of 833 cm^{-1}.[38] The two main bands of 1619 and 1498 cm^{-1} were respectively assigned to C=C stretching vibrations in quinoid and benzenoid rings. It can be seen that the peak at 1619 cm^{-1} of Pd/polyaniline/CFC became stronger while that at 1498 cm^{-1} was weaker compared with the peaks of polyaniline/CFC. It was elucidated that after modification of Pd, polyaniline was oxidized from PAN_{re} to PAN_{ox} with more quinoid and less benzenoid units.

XRD was introduced to confirm the existence of crystalline Pd. In Fig. 5a, the CFC displayed three broad peaks centered at about 23°, 43° and 80°, which can be attributed to carbon. The characteristic peaks of polyaniline probably overlapped with that of CFC and thus, polyaniline cannot be identified in XRD profiles. After the polyaniline/CFC was modified by Pd, there were five diffraction peaks at 40°, 47°, 68°, 82° and 87°, corresponding well to the (111), (200) and (220), (311) and (222) planes of Pd, respectively, according to the standard crystallographic spectrum of Pd (JCPDS card No. 46-1043).

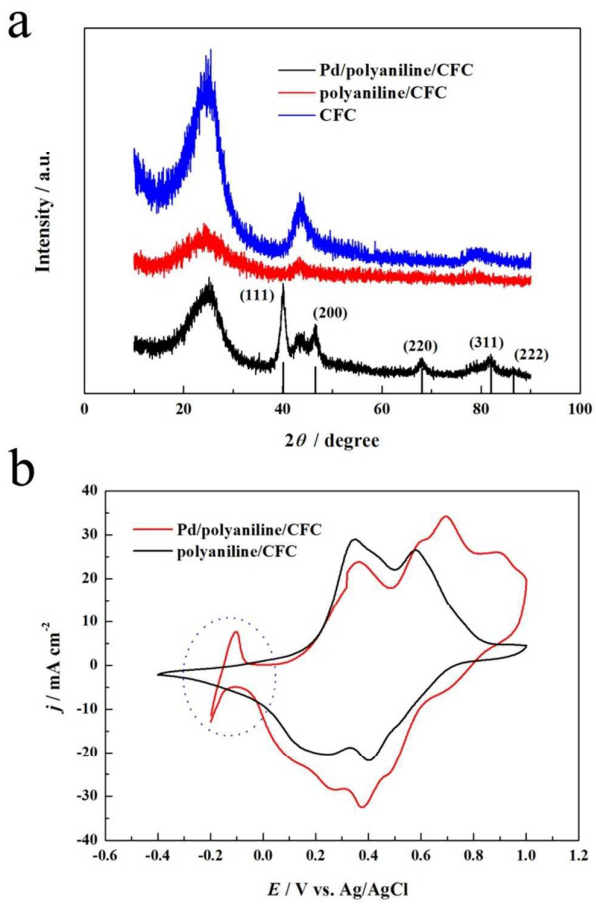

Fig. 5 (a) XRD patterns of CFC, polyaniline/CFC and Pd/polyaniline/CFC electrode; (b) cyclic voltammograms of polyaniline/CFC and Pd/polyaniline/CFC electrode in 1.0 mol L^{-1} H_2SO_4 at 10 mV s^{-1}.

These peaks indicated that Pd modified on polyaniline had a face-centered cubic (fcc) structure and presented as the metallic state. The FTIR and XRD patterns manifested that binder-free and self-catalytic reductive Pd/polyaniline/CFC electrode was successfully fabricated. Fig. 5b shows the cyclic voltammograms (CV) of the polyaniline/CFC and Pd/polyaniline/CFC electrode measured in 1.0 mol L^{-1} H_2SO_4 at scan rate of 10 mV s^{-1}, respectively. The CV curve of polyaniline/CFC exhibited two pair of redox peaks between –0.4 V and 1.0 V, due to the conversions of Emeraldine/lencomeraldine and lencomeraldine/pernigraniline. The CV of Pd/polyaniline/CFC displayed the absorption and/or evolution of hydrogen region from –0.1 V to –0.2 V and hydrogen desorption region at –0.08 V, which were the typical features of Pd[39]. Due to the metallic Pd oxidation and reduction reactions in H_2SO_4[40], compared with polyaniline/CFC electrode, the current density of Pd/polyaniline/CFC between the potential ranges of 0.6–1.0 V and 0–0.8 V was larger. The CV of Pd/polyaniline/CFC emerged more couples of redox peaks than that of polyaniline/CFC, inferring that Pd modification could facilitate the successive conversions of more redox states of polyaniline.

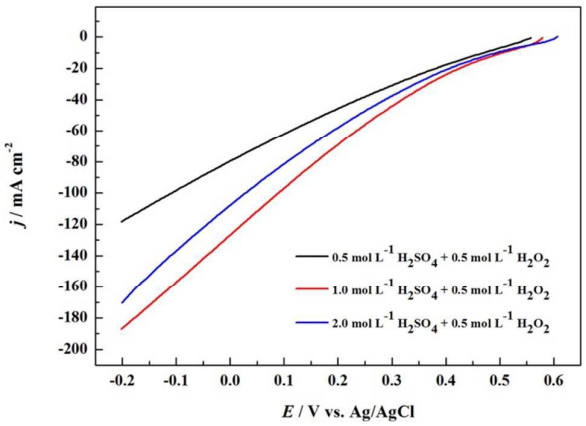

Fig. 6 Linear sweep voltammograms of Pd/polyaniline/CFC electrode in different concentrations of H_2SO_4 in the presence of 0.5 mol L^{-1} H_2O_2 at a scan rate of 10 mV s^{-1}.

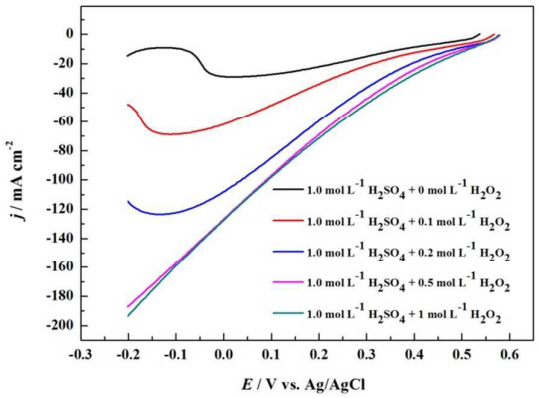

Fig. 7 Linear sweep voltammograms of Pd/polyaniline/CFC electrode in the different concentrations of H_2O_2 with the presence of 1.0 mol L^{-1} H_2SO_4 at a scan rate of 10 mV s^{-1}.

Fig. 6 demonstrates the linear sweep voltammograms (LSVs) of Pd/polyaniline/CFC electrode in 0.5 mol L^{-1} H_2O_2 and *x* mol L^{-1} H_2SO_4 (*x*= 0.5, 1.0, 2.0). The potential applied to the Pd/polyaniline electrode was swept from open circuit potential (OCP) to –0.2 V at a scan rate of 10 mV s^{-1}. With the concentration of H_2SO_4 increasing from 0.5 mol L^{-1} to 2.0 mol L^{-1}, the OCP moved positively from 0.558 V to 0.608 V. The OCP shift trend was in accordance with the previous literatures on Pd electrode for H_2O_2 electro-reduction[40, 41]. The Pd/polyaniline/CFC revealed the best performance in 1.0 mol L^{-1} H_2SO_4 and 0.5 mol L^{-1} H_2O_2 according to the current density. The current density at -0.2 V was 189 mA cm^{-2} with an OCP of 0.580 V. As known, the function of H_2SO_4 is not just the supporting electrolyte, it is a reactant that reacted with H_2O_2 at the chemical ingredient ratio of 2:1 ($H_2O_2+2H^++2e^- \rightleftarrows 2H_2O$). As a result, inadequate (0.5 mol L^{-1}, 1:1 stoichiometry) and excess (2.0 mol L^{-1}, 4:1 stoichiometry) H_2SO_4 at fixed concentration of H_2O_2 would both suppressed the H_2O_2 electro-reduction reaction on Pd/polyaniline/CFC electrode.

Fig. 7 shows the effects of H_2O_2 concentration on the catalytic behavior of Pd/polyaniline/CFC electrode. The concentration of H_2SO_4 was fixed at 1.0 mol L^{-1}. As seen, the OCP increased from 0 to 0.2 mol L^{-1} H_2O_2 and then remained unchanged even at a high concentration of 1.0 mol L^{-1}. Cao et al.[41] analyzed the influence of H_2O_2 concentration on the OCPs at a variety of electrodes in 1.0 mol L^{-1} H_2SO_4. Each electrode had its own OCP trend. The OCP at Pd electrode stepped up from 0.02 to 0.1 mol L^{-1} and then almost did not change from 0.1 to 1.0 mol L^{-1}. The Pd/polyaniline/CFC had the same OCP tendency with Pd electrode in different concentration of H_2SO_4 and H_2O_2, meaning that equilibrium state of H_2O_2 electro-reduction was mostly established on the modified Pd, and so proceeded the sequent electro-reduction process. Without any addition of H_2O_2, the LSV of Pd/polyaniline/CFC showed the reduction current of polyaniline and hydrogen absorption in H_2SO_4. The reduction peak of H_2O_2 diminished gradually and disappeared from 0.1 to 0.5 mol L^{-1}, since more H_2O_2 content reduced the concentration polarization. When the concentration of H_2O_2 further increased to 1.0 mol L^{-1}, the current density at –0.2 V was 195 mA cm^{-2}, only 6 mA cm^{-2} larger than that of 0.5 mol L^{-1}. Taking into account the fuel costs, 0.5 mol L^{-1} was considered as the optimal concentration of H_2O_2.

The stability of polyaniline/CFC and Pd/polyaniline/CFC electrode in 1.0 mol L^{-1} H_2SO_4 and 0.5 mol L^{-1} H_2O_2 was tested by applying different polarization potentials. The current-time curves are depicted in Fig. 8. Starting from 0.4 V, the polarization potential was decreased to –0.2 V by three steps and held for 30 minutes at each potential. As seen, the lower the potential, the larger the reduction current density. The current densities were almost kept constant at 0.4 V (14 mA cm^{-2}) and 0.1 V (75 mA cm^{-2}). The current density at –0.2 V on Pd/polyaniline/CFC electrode delivered slight decrease from 166 mA cm^{-2} at 3721 s to 157 mA cm^{-2} at 5400 s during the 1800s testing time, which is likely resulted from the

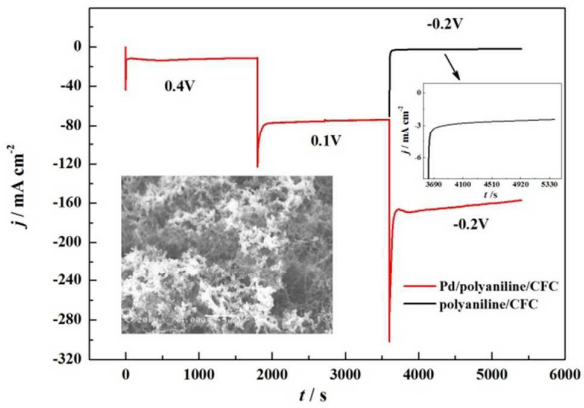

Fig. 8 Chronoamperometric curves of polyaniline/CFC and Pd/polyaniline/CFC electrode for H_2O_2 electro-reduction at different potentials in 1.0 mol L^{-1} H_2SO_4 and 0.5 mol L^{-1} H_2O_2. Inset (left) is the SEM image of Pd/polyaniline/CFC electrode after chronoamperometric test; inset(right) is the enlarged *i-t* curve of polyaniline/CFC electrode at -0.2 V in 1.0 mol L^{-1} H_2SO_4 and 0.5 mol L^{-1} H_2O_2.

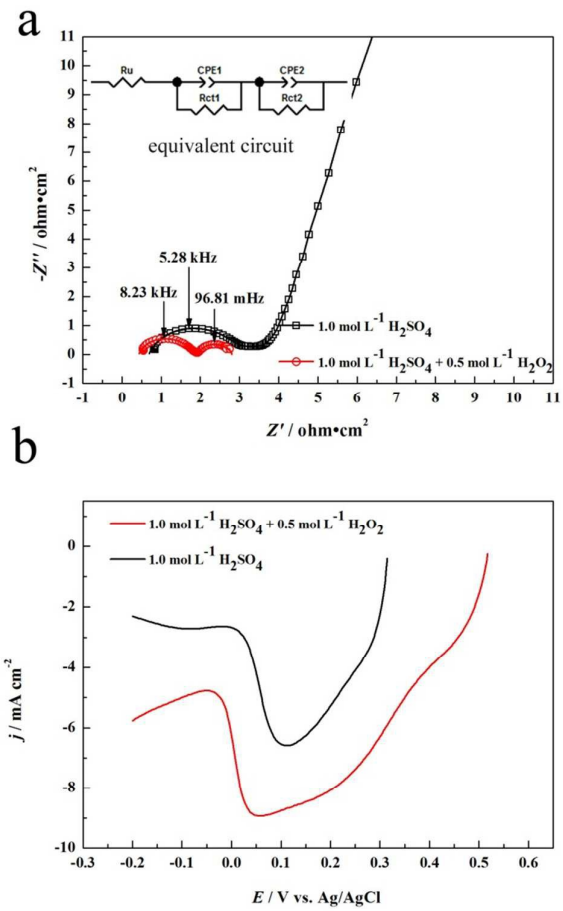

Fig. 9 (a) Nyquist plots of Pd/polyaniline/CFC electrode at 0.1 V in 1.0 mol L^{-1} H_2SO_4 in the absence and presence of 0.5 mol L^{-1} H_2O_2, inset is the equivalent circuit of polyaniline and H_2O_2 electro-reduction on Pd/polyaniline/CFC electrode; (b) linear sweep voltammograms of polyaniline/CFC electrode in 1.0 mol L^{-1} H_2SO_4 with and without 0.5 mol L^{-1} H_2O_2 at 10 mV s^{-1}.

consumption of H_2O_2 near the electrode surface. Polyaniline/CFC electrode was also tested in 1.0 mol L^{-1} H_2SO_4 and 0.5 mol L^{-1} H_2O_2 at –0.2 V. It demonstrated a low current density of ~3.0 mA cm^{-2}, nearly negligible compared with Pd/polyaniline/CFC electrode. The low current density was probably resulted from the reduction of polyaniline. Inset (left) of Fig. 8 is the SEM image of Pd/polyaniline/CFC electrode after choronoamperometric test. The morphologys of polyaniline fibrils and Pd particles were well retained. In conclusion, the Pd/polyaniline/CFC electrode exhibited excellent stability for H_2O_2 electro-reduction reaction because of the synergistic properties of high-surface-area polyaniline doping-dedoping in H_2SO_4 and Pd electro-reduction towards H_2O_2.

Fig. 9a illustrates the Nyquist plots of Pd/polyaniline/CFC electrode at 0.1 V containing 1.0 mol L^{-1} H_2SO_4 with and without 0.5 mol L^{-1} H_2O_2, respectively. The electrochemical system was first polarized for 600 s at 0.1 V to achieve quasi-stable state. In the absence of H_2O_2, when only polyaniline was electro-reduced, one depressed semi-circle in the higher frequency region and a spike in lower frequency region appeared. After adding H_2O_2, there were two depressed semi-circles. One in the higher frequency region was ascribed to the electro-reduction reaction of polyaniline, since the frequency of first circle, 8.23 kHz, is very close to that without H_2O_2, 5.28 kHz[10, 42]. The other circle with a frequency of 96.81 mHz was attributed to the H_2O_2 electro-reduction reaction on Pd with a diameter of 0.876 Ω (R_{ct2}). Inset of Fig. 9a is the equivalent circuit of both polyaniline electro-reduction and H_2O_2 electro-reduction on Pd. H_2O_2 electro-reduction (R_{ct2}) happened in parallel with polyaniline reduction (R_{ct1}). In comparison with the semi-circle without H_2O_2, the ohmic resistance (R_u) of that with H_2O_2 was smaller, this could be because of the increased solution and/or polyaniline conductivity after adding H_2O_2. The diameter of the semi-circle was charge transfer resistance (R_{ct}), which could be used to evaluate the electrochemical reaction rate. R_{ct1} of polyaniline (1.372 Ω) electro-reduction in H_2SO_4 and H_2O_2 was smaller than that (2.342 Ω) only in H_2SO_4, implying the addition of H_2O_2 facilitated the polyaniline electro-reduction reaction. To further gain the understanding of interaction between polyaniline and H_2O_2, the CV synthesized polyaniline was solely tested in 1.0 mol L^{-1} H_2SO_4 with and without 0.5 mol L^{-1} H_2O_2. As shown in Fig. 9b, the OCP of polyaniline electrode changed from 0.31 V to 0.51 V. The positive shift of OCP implied that polyaniline was oxidized after adding H_2O_2. The amplitude of reduction current density was increased after adding H_2O_2. It was demonstrated that polyaniline itself showed electro-catalytic activity towards H_2O_2 to some extent. It could be speculated that H_2O_2 electrode-reduction on polyaniline proceeded in a way of chemical-electrochemical process (C-E process).

Chemical process:

$$PAN_{re} + H_2O_2 + 2H_2SO_4 \rightleftarrows PAN_{ox}^{+}\bullet 2HSO_4^{-} + 2H_2O \quad (3)$$

Electrochemical process:

$$PAN_{ox}^{+}\bullet 2HSO_4^{-} + 2e^{-} \rightleftarrows PAN_{re} + 2HSO_4^{-} \quad (4)$$

Overall reaction

$$H_2O_2 + 2H^{+} + 2e^{-} \rightleftarrows 2H_2O \quad (3)+(4)$$

Polyaniline was first chemical-oxidized to its oxidation state by H_2O_2 (chemical process), and then electrochemical-reduced to its reduction state by external potential driving force (electrochemical process). As a result, the overall reaction turned out that H_2O_2 was electro-reduced to H_2O on the polyaniline electrode. The C-E coupling mechanism was commonly seen on the Cu_2O and Pt electrodes for H_2O_2 electro-reduction or electro-oxidation[43–45] as well.

4. Conclusions

In conclusion, the binder-free Pd/polyaniline/CFC electrode was successfully prepared based on the equilibrium potential difference between Pd complex ions and CV synthesized polyaniline. The size of Pd particles coated on polyaniline networks gradiently distributed from the outside to inside. The modified Pd/polyaniline/CFC electrode demonstrated high catalytic activity and remarkable stability towards H_2O_2 electro-reduction in sulfuric acid even at relatively negative potentials.

Polyaniline solely exhibited electro-catalytic activity for H_2O_2 electro-reduction in a way of chemical-electrochemical coupling process.

Acknowledgements

We gratefully acknowledge the financial support of this research by the National Natural Science Foundation of China (21403044), the Natural Science Foundation of Heilongjiang Province of China (LC2015004), the China Postdoctoral Science Special Foundation (2015T80329), the Heilongjiang Postdoctoral Fund (LBH-Z14211), the China Postdoctoral Science Foundation (2014M561332), the Major Project of Science and Technology of Heilongjiang Province (GA14A101), the Project of Research and Development of Applied Technology of Harbin (2014DB4AG016) and the Fundamental Research Funds for the Central Universities (HEUCF20151004).

Notes and references

1 Y. Pan, K. Ye, D. Cao, Y. Li, Y. Dong, T. Niu, W. Zeng and G. Wang, Nitrogen-doped graphene oxide/cupric oxide as an anode material for lithium ion batteries, *RSC Adv.*, 2014, **4**, 64756–64762.

2 P. Xu, K. Ye, M. Du, J. Liu, K. Cheng, J. Yin, G. Wang and D. Cao, One-step synthesis of copper compounds on copper foil and their supercapacitive performance, *RSC Adv.*, 2015, **5**, 36656–36664.

3 P. Xu, K. Ye, D. Cao, J. Huang, T. Liu, K. Cheng, J. Yin and G. Wang, Facile synthesis of cobalt manganese oxides nanowires on nickel foam with superior electrochemical performance, *J. Power Sources*, 2014, **268**, 204–211.

4 T. Zhou, R. Shao, S. Chen, X. He, J. Qiao and J. Zhang, A review of radiation-grafted polymer electrolyte membranes for alkaline polymer electrolyte membrane fuel cells, *J. Power Sources*, 2015, **293**, 946–975.

5 S. P. S. Badwal, S. Giddey, A. Kulkarni, J. Goel and S. Basu, Direct ethanol fuel cells for transport and stationary applications–A comprehensive review, *Appl. Energ.*, 2015, **145**, 80–103.

6 K. Ye, Y. Aoki, E. Tsuji, S. Nagata and H. Habazaki, Thickness dependence of proton conductivity of anodic ZrO_2-WO_3-SiO_2 nanofilms, *J. Power Sources*, 2012, **205**, 194–200.

7 F. Guo, K. Ye, K. Cheng, G. Wang and D. Cao, Preparation of nickel nanowire arrays electrode for urea electrooxidation in alkaline medium, *J. Power Sources*, 2015, **278**, 562–568.

8 C. Shu, E. Wang, L. Jiang, Q. Tang and G. Sun, Studies on palladium coated titanium foams cathode for Mg–H_2O_2 fuel cells, *J. Power Sources*, 2012, **208**, 159–164.

9 L. Yi, W. Wei, C. Zhao, L. Tian, J. Liu and X. Wang, Enhanced activity of Au-Fe/C anodic electrocatalyst for direct borohydride-hydrogen peroxide fuel cell, *J. Power Sources*, 2015, **285**, 325–333.

10 K. Ye, F. Guo, Y. Gao, D. Zhang, K. Cheng, W. Zhang, G. Wang and D. Cao, Three-dimensional carbon- and binder-free nickel nanowire arrays as a high-performance and low-cost anode for direct hydrogen peroxide fuel cell, *J. Power Sources*, 2015, **300**, 147–156.

11 S. J. Lao, H. Y. Qin, L. Q. Ye, B. H. Liu and Z. P. Li, A development of direct hydrazine/hydrogen peroxide fuel cell, *J. Power Sources*, 2010, **195**, 4135–4138.

12 K. Ye, D. Zhang, H. Zhang, K. Cheng, G. Wang and D. Cao, Platinum-modified cobalt nanosheets supported on three-dimensional carbon sponge as a high-performance catalyst for hydrogen peroxide electroreduction, *Electrochim. Acta*, 2015, **178**, 270–279.

13 K. Ye, D. Zhang, X. Wang, K. Cheng and D. Cao, A novel three-dimensional gold catalyst prepared by simple pulse electrodeposition and its high electrochemical performance for hydrogen peroxide reduction, *RSC Adv.*, 2015, **5**, 3239–3247.

14 S. J. Pomfret, P. N. Adams, N. P. Comfort and A. P. Monkman, Inherently electrically conductive fibers wet spun from a sulfonic acid-doped polyaniline solution, *Adv. Mater.*, 1998, **10**, 1351–1353.

15 K. B. Jirage, J. C. Hulteen and C. R. Martin, Nanotubule-based molecular-filtration membranes, *Science*, 1997, **278**, 655–658.

16 P. A. Hassan, S. N. Sawant, N. C. Bagkar and J. V. Yakhmi, Polyaniline nanoparticles prepared in rodlike micelles, *Langmuir*, 2004, **20**, 4874–4880.

17 Z. Niu, Z. Yang, Z. Hu, Y. Lu and C. C. Han, Polyaniline-silica composite conductive capsules and hollow spheres, *Adv. Funct. Mater.*, 2003, **13**, 949–954.

18 C. Coutanceau, M. J. Croissant, T. Napporn and C. Lamy, Electrocatalytic reduction of dioxygen at platinum particles dispersed in a polyaniline film, *Electrochim. Acta*, 2000, **46**, 579–588.

19 N. V. Blinova, J. Stejskal, M. Trchová, I. Sapurina and G. Ćirić-Marjanović, The oxidation of aniline with silver nitrate to polyaniline-silver composites, *Polymer*, 2009, **50**, 50–56.

20 H. Zhang, F. Huang, S. Xu, Y. Xia, W. Huang and Z. Li, Fabrication of nanoflower-like dendritic Au and polyaniline composite nanosheets at gas/liquid interface for electrocatalytic oxidation and sensing of ascorbic acid, *Electrochem. Commun.*, 2013, **30**, 46–50.

21 D. Zhang, D. Cao, K. Ye, J. Yin, K. Cheng and G. Wang, Cobalt nano-sheet supported on graphite modified paper as a binder free electrode for peroxide electrooxidation, *Electrochim. Acta*, 2014, **139**, 250–255.

22 K. Ye, D. Zhang, F. Guo, K. Cheng, G. Wang and D. Cao, Highly porous nickel@carbon sponge as a novel type of three-dimensional anode with low cost for high catalytic performance of urea electro-oxidation in alkaline medium, *J. Power Sources*, 2015, **283**, 408–415.

23 X. Cheng, K. Ye, D. Zhang, K. Cheng, Y. Li, B. Wang, G. Wang and D. Cao, Methanol electrooxidation on flexible multi-walled carbon nanotube-modified sponge-based nickel electrode, *J. Solid State Electrochem.*, 2015, **19**, 3027–3034.

24 L. Niu, Q. Li, F. Wei, X. Chen and H. Wang, Formation optimization of platinum-modified polyaniline films for the electrocatalytic oxidation of methanol, *Synthetic Met.*, 2003, **139**, 271–276.

25 L. Niu, Q. Li, F. Wei, X. Chen and H. Wang, Electrochemical impedance and morphological characterization of platinum-modified polyaniline film electrodes and their electrocatalytic activity for methanol oxidation, *J. Electroanal. Chem.*, 2003, **544**, 121–128.

26 W. S. Huang, B. D. Humphrey and A. G. MacDiarmid, Polyaniline, a novel conducting polymer morphology and chemistry of its oxidation and reduction in aqueous electrolytes, *J. Chem. Soc., Faraday Trans. 1*, 1986, **82**, 2385–2400.

27 M. Hosseini and M. M. Momeni, Silver nanoparticles dispersed in polyaniline matrixes coated on titanium substrate as a novel electrode for electro-oxidation of hydrazine, *J. Mater. Sci.*, 2010, **45**, 3304–3310.

28 K. M. Kost, D. E. Bartak, B. Kazee and T. Kuwana, Electrodeposition of platinum microparticles into polyaniline films with electrocatalytic applications, *Anal. Chem.*, 1988, **60**, 2379–2384.
29 A. G. Macdiarmid, J. C. Chiang, W. Huang, B. D. Humphrey and N. L. D. Somasiri, Polyaniline: protonic acid doping to the metallic regime, *Mol. Cryst. Liq. Cryst.*, 1985, **125**, 309–318.
30 A. N. Grace and K. Pandian, Pt, Pt-Pd and Pt-Pd/Ru nanoparticles entrapped polyaniline electrodes–A potent electrocatalyst towards the oxidation of glycerol, *Electrochem. Commun.*, 2006, **8**, 1340–1348.
31 Z. Gao, W. Yang, J. Wang, H. Yan, Y. Yao, J. Ma, B. Wang, M. Zhang and L. Liu, Electrochemical synthesis of layer-by-layer reduced graphene oxide sheets/polyaniline nanofibers composite and its electrochemical performance, *Electrochim. Acta*, 2013, **91**, 185–194.
32 A. Mourato, A. S. Viana, J. P. Correia, H. Siegenthaler and L. M. Abrantes, Polyaniline films containing electrolessly precipitated palladium, *Electrochim. Acta*, 2004, **49**, 2249–2257.
33 H. G. Lemos, S. F. Santos and E. C. Venancio, Polyaniline-Pt and polypyrrole-Pt nanocomposites: Effect of supporting type and morphology on the nanoparticles size and distribution, *Synthetic Met.*, 2015, **203**, 22–30.
34 R. Yan and B. Jin, Preparation and electrochemical performance of polyaniline/Pt microelectrodes, *Electrochim. Acta*, 2014, **115**, 449–453.
35 N. Elhalawany, H. Elmelegy and M. Nayfeh, Synthesis, characterization and electrical properties of highly conductive polyaniline/gold and/or platinum nanocomposites, *Synthetic Met.*, 2015, **205**, 145–152.
36 E. T. Kang, K. G. Neoh and K. L. Tan, Polyaniline: a polymer with many interesting intrinsic redox states, *Prog. Polym. Sci.*, 1998, **23**, 277–324.
37 Y. H. Kim, C. Foster, J. Chiang and A. J. Heeger, Photoinduced localized charged excitations in polyaniline, *Synthetic Met.*, 1988, **26**, 49–59.
38 M. Trchová, I. Šeděnková, E. Tobolková and J. Stejskal, FTIR spectroscopic and conductivity study of the thermal degradation of polyaniline films, *Polym. Degrad. Stabil.*, 2004, **86**, 179–185.
39 J. P. Chevillot, J. Farcy, C. Hinnen and A. Rousseau, Electrochemical study of hydrogen interaction with palladium and platinum, *J. Electroanal. Chem. Interfacial Electrochem.*, 1975, **64**, 39–62.
40 D. Cao, L. Sun, G. Wang, Y. Lv and M. Zhang, Kinetics of hydrogen peroxide electroreduction on Pd nanoparticles in acidic medium, *J. Electroanal. Chem.*, 2008, **621**, 31–37.
41 X. Jing, D. Cao, Y. Liu, G. Wang, J. Yin, Q. Wen and Y. Gao, The open circuit potential of hydrogen peroxide at noble and glassy carbon electrodes in acidic and basic electrolytes, *J. Electroanal. Chem.*, 2011, **658**, 46–51.
42 K. Ye, Y. Aoki, E. Tsuji, S. Nagata and H. Habazaki, Improved Thermal Stability of Efficient Proton-Conducting Anodic ZrO_2-WO_3 Nanofilms by Incorporation of Silicon Species, *J. Electrochem. Soc.*, 2011, **158**, C385–C390.
43 K. L. Stewart and A. A. Gewirth, Mechanism of electrochemical reduction of hydrogen peroxide on copper in acidic sulfate solutions, *Langmuir*, 2007, **23**, 9911–9918.
44 T. Selvaraju and R. Ramaraj, Electrocatalytic reduction of hydrogen peroxide at nanostructured copper modified electrode, *J. Appl. Electrochem.*, 2009, **39**, 321–327.
45 J. S. Goldik, J. J. Noël and D. W. Shoesmith, The electrochemical reduction of hydrogen peroxide on uranium dioxide electrodes in alkaline solution, *J. Electroanal. Chem.*, 2005, **582**, 241–248.